极亮X射线源的星族合成研究

汇报人：物试72 宋昊天

日　期：2021年4月

目录
content

1 背景介绍

研究基础

西安交通大學
XI'AN JIAOTONG UNIVERSITY

国内外研究现状

ultra-luminous X-ray sources (ULXs)是指光度超过$10^{39} erg/s$的X射线点源

因为其超过了Eddington 亮度所以受到广泛关注

现阶段认为ULXs的主要产生机理为洛希瓣吸积(RLOF)

研究基础

国内外研究现状

现阶段针对ULX的星族合成模拟主要有：

Yong Shao et al 2019

针对Helium Star进行了星族模拟，仅考虑RLOF

Wiktorowicz et al 2021

仅考虑了red supergiants (RSGs)，运用的WRL吸积模型对伴星质量有限制。

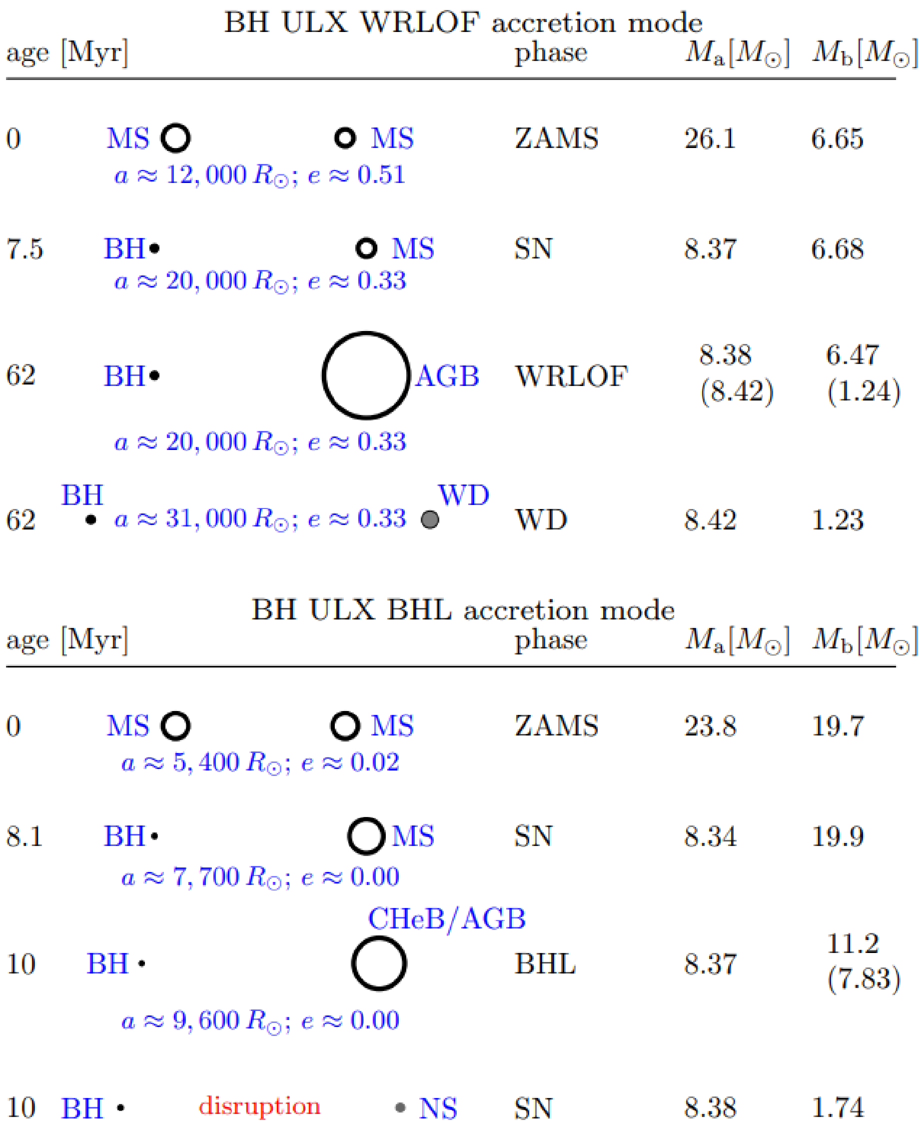

Wiktorowicz et al 2021

XI'AN JIAOTONG UNIVERSITY 西安交通大學

2

项目进展

项目进展

项目创新点

1，在星族合成中采用各向异性的风吸积模型

（El Mellah et al 2019）

2，创新性采用星暴星系的相关观测结果来论证星族合成模拟的结果（Wolter et al 2018）

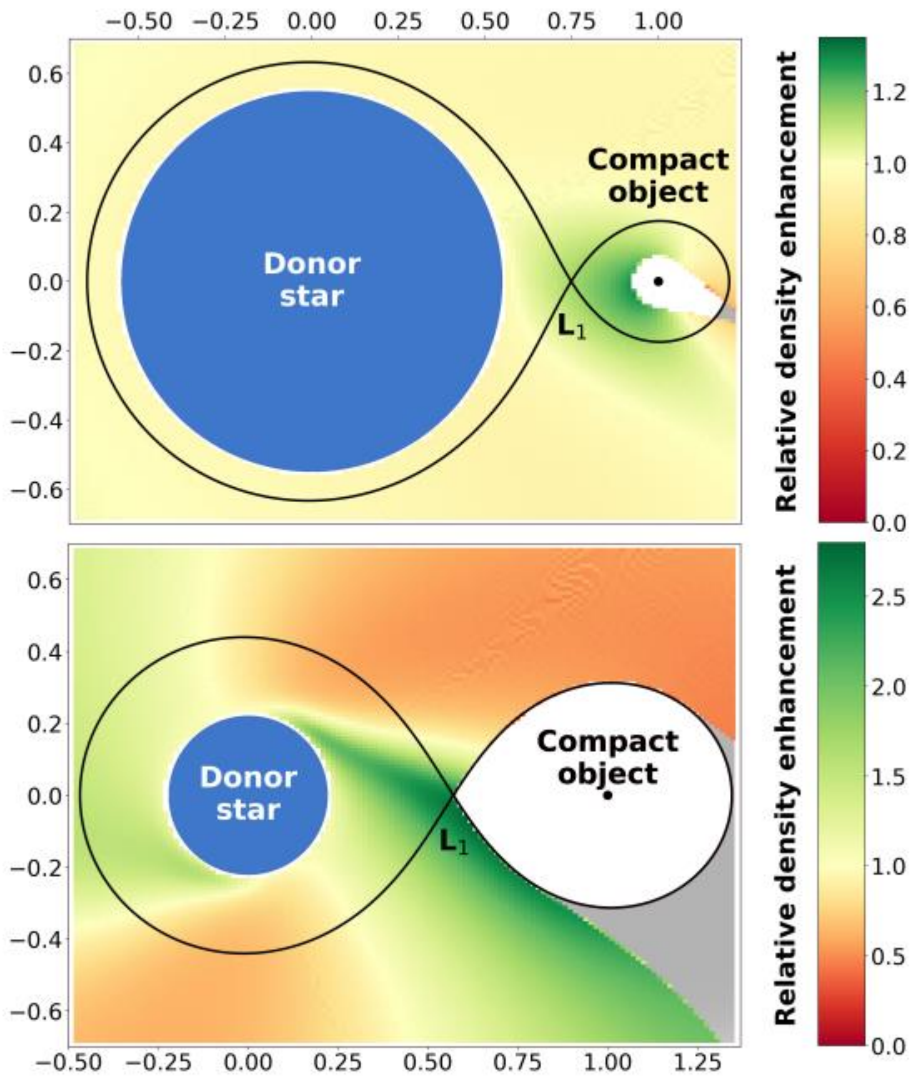

El Mellah et al 2019

项目进展

模型设置

1，针对充满洛希瓣的风吸积，我们采用数值模拟的结果计算吸积效率

2，针对洛希瓣吸积，采用beaming模型（各向异性X射线辐射）来进行光度计算

$$L_{app} = L_x/b$$

3，用mesa对中子星为主星进行更细致的演化计算

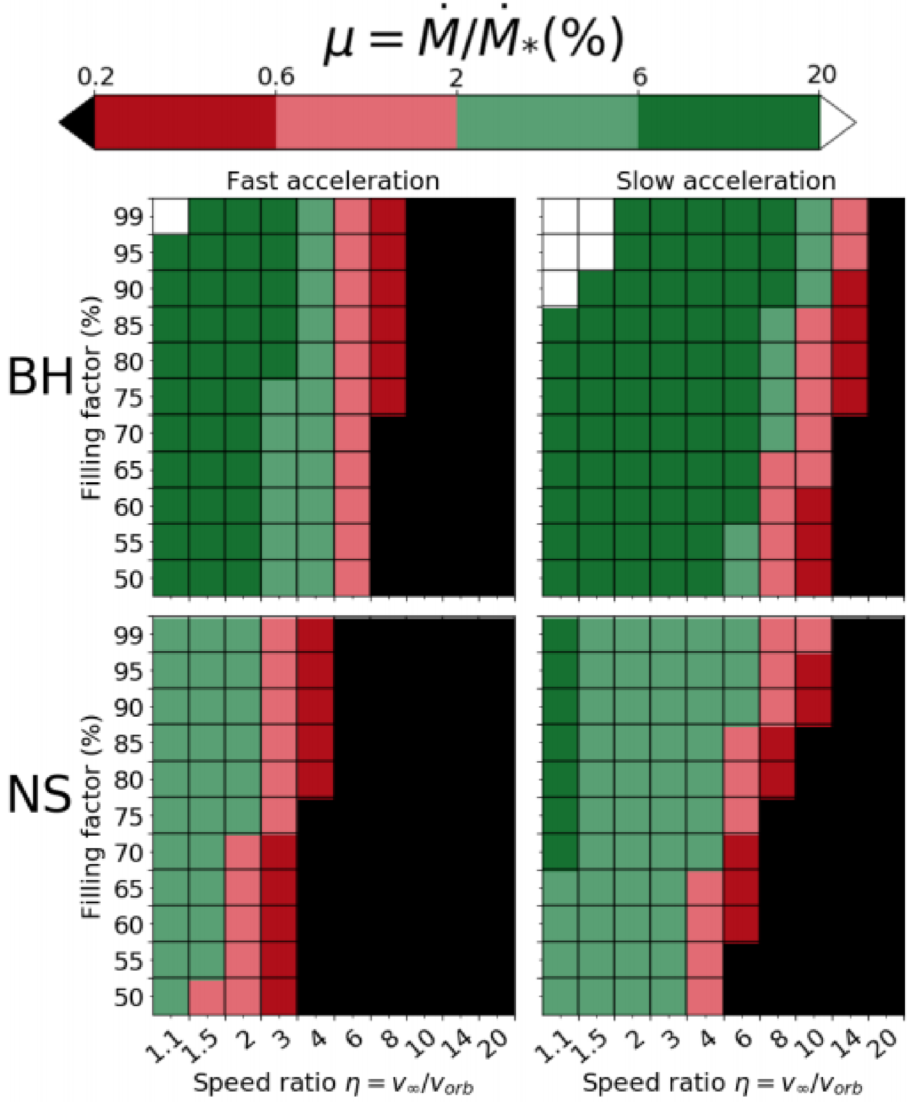

El Mellah et al 2019

项目进展

计算结果

我们把光度函数（XLF）与观测结果（图中红点）进行比较

与观测基本吻合

星族成分基本上是黑洞在低光度时占主导

中子星在高光度时占主导

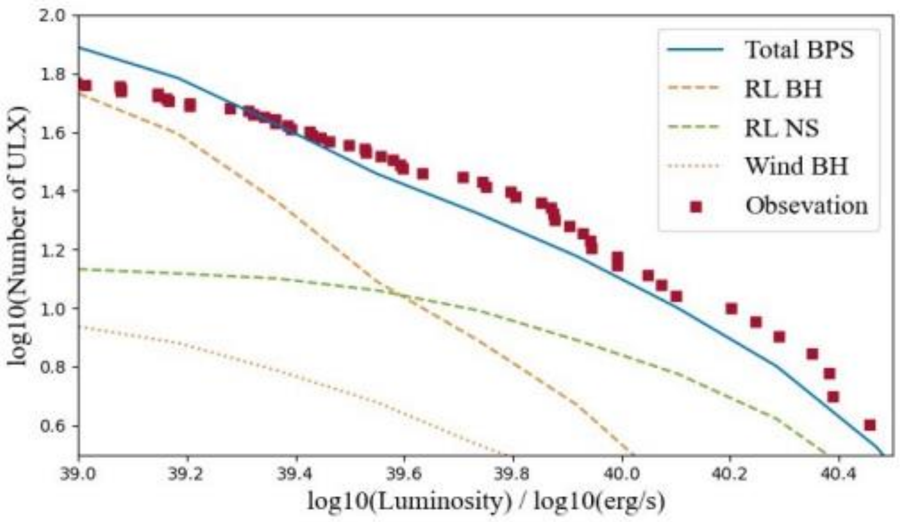

(a)

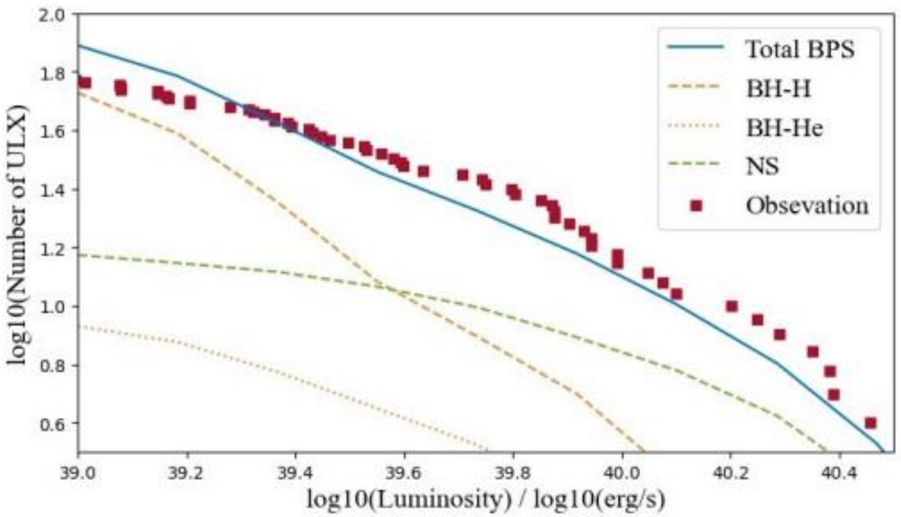

(b)

项目进展

计算结果

不同演化时间的分析

因为是星暴星系，恒星一般比较年轻，所以计算时间都是200Myr以下

(Wolter et al 2018)

非常年轻的星占比较少，也很难达到高光度的情况

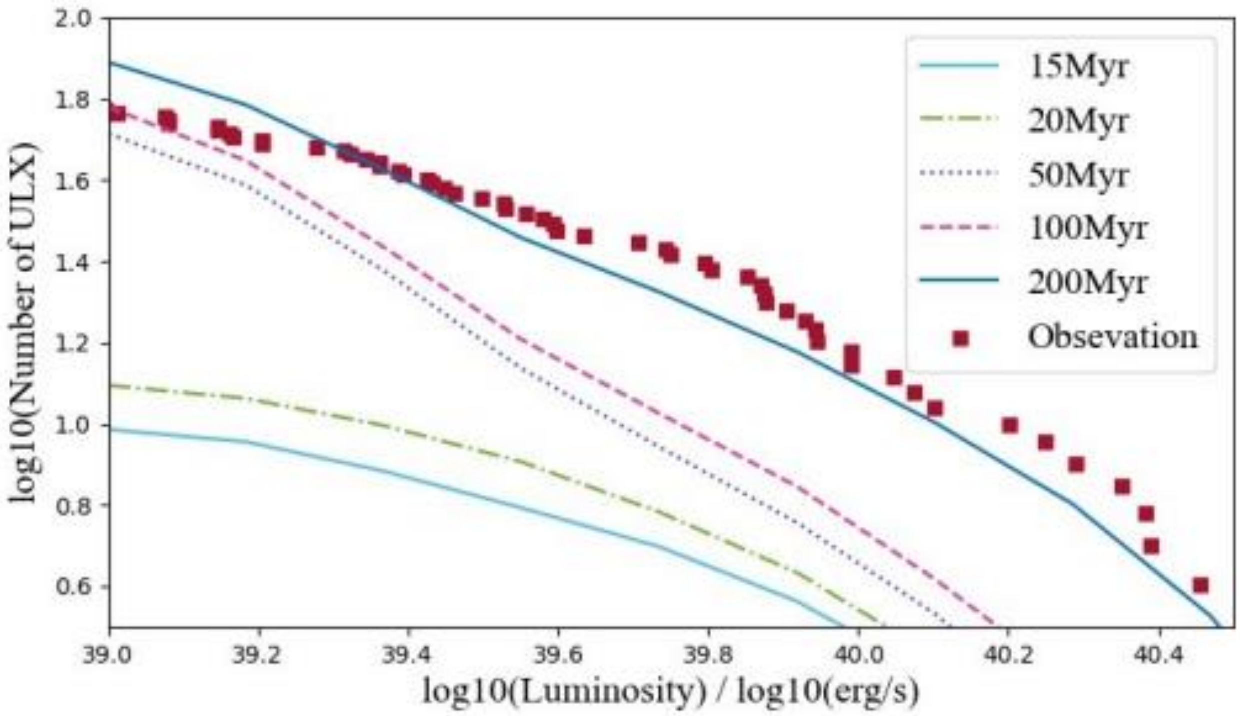

Figure 2. XLF for various evolution duration of ULXs for 200 Myr, 100 Myr, 50 Myr, 20 Myr, 15 Myr.

3

未来展望

未来展望

需要解决的问题

1，细致的星族分析，包括质量轨道平面的各个板块的星族构成

2，双星演化路径的进一步确定，得出主要的恒星演化路径

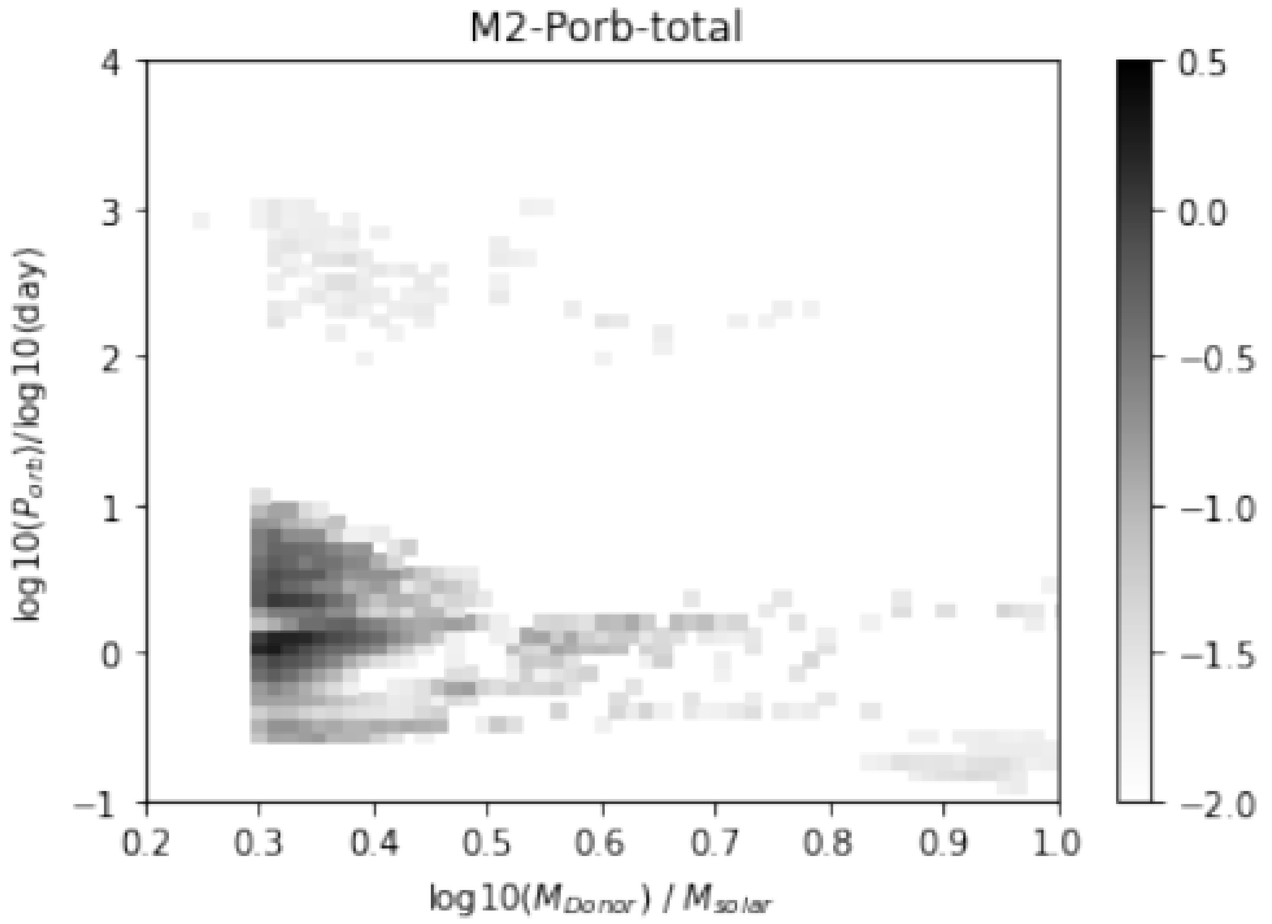

参考文献

Wolter, A. et al., 2018, ApJ, 863, 43
El Mellah, I. et al., 2019, A&A, 622, L3
Hurley J. R., Pols O. R., Tout C. A., 2000, MNRAS, 315, 543
Hurley J. R., Tout C. A., Pols O. R., 2002, MNRAS, 329, 897
Shao Y., Li X. D., 2015, Astrophysical Journal, 802
Shao Y., Li X.-D., Dai Z.-G., 2019, ApJ , 886, 118
Wiktorowicz G., Lasota J.-P., Middleton M., Belczynski K., 2019a, The Astrophysical Journal, 875, 53
Wiktorowicz G., Lasota J.-P., Middleton M., Belczynski K., 2019b, The Astrophysical Journal, 875, 53
Wiktorowicz G., Sobolewska M., Lasota J.-P., Belczynski K., 2017, The Astrophysical Journal, 846, 17
King A., 2008, Monthly Notices of the Royal Astronomical Society: Letters, 385, L113
King A., 2009, Monthly Notices of the Royal Astronomical Society: Letters, 393, L41
Abate C., Pols O. R., Izzard R. G., Mohamed S. S., de Mink S. E., 2013, A&A , 552, A26

谢谢大家！

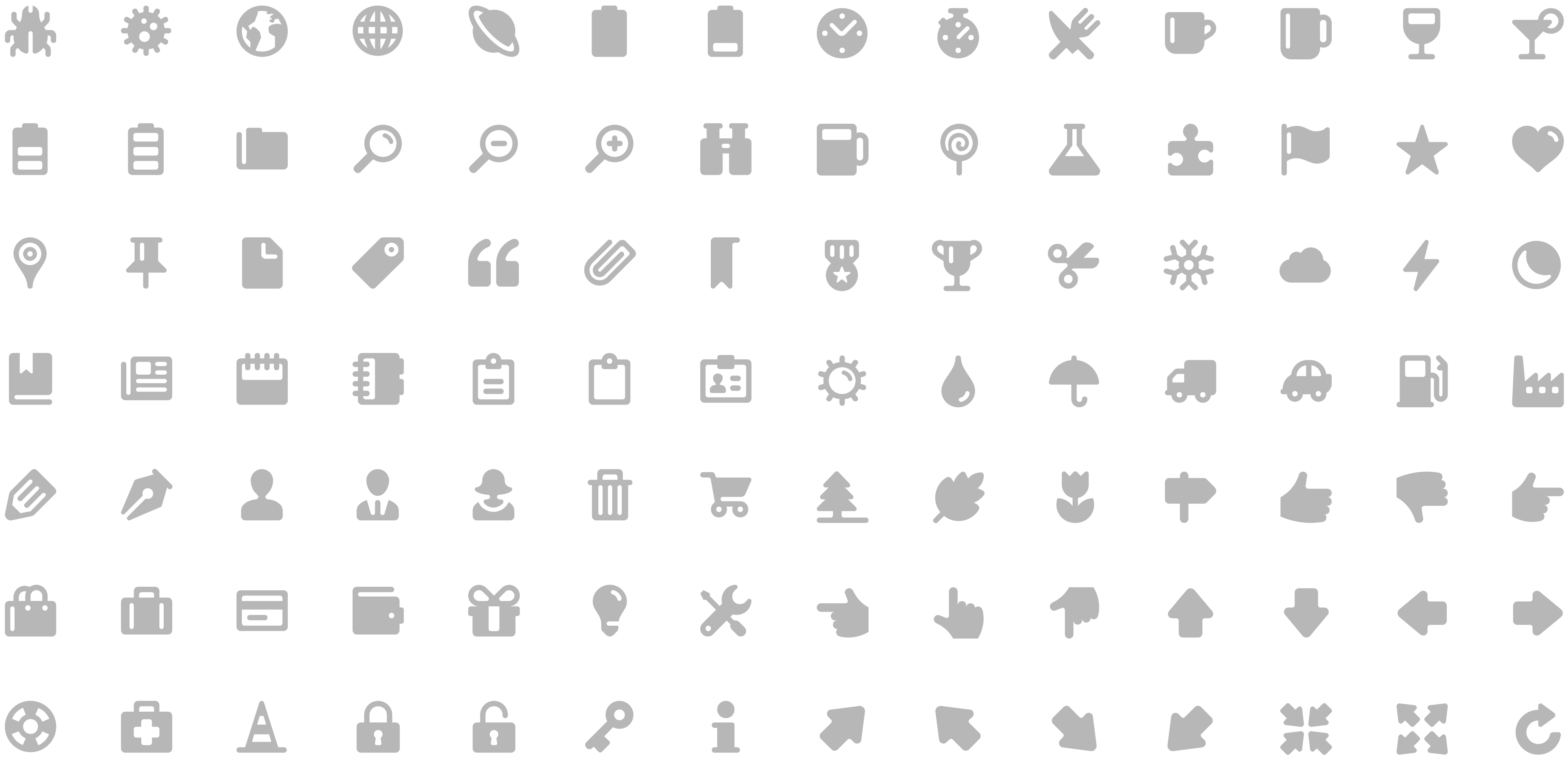

附录

Star-burst galaxies

The reason of burst star forming in Ring Galaxies is encounter with nearby galaxies

1, the age of stars is similar.

2, most ULXs formulation environment is normal sharing similar metallicity Wolter et al. (2018).

3, with high star forming rates (SFR) and shorter evolution duration, Ring Galaxies share more similarity with assuming environment, which avoids the various initial conditions of EPS

4, remarkable number of ULXs was detected in Star-burst galaxies strongly supports our simulation

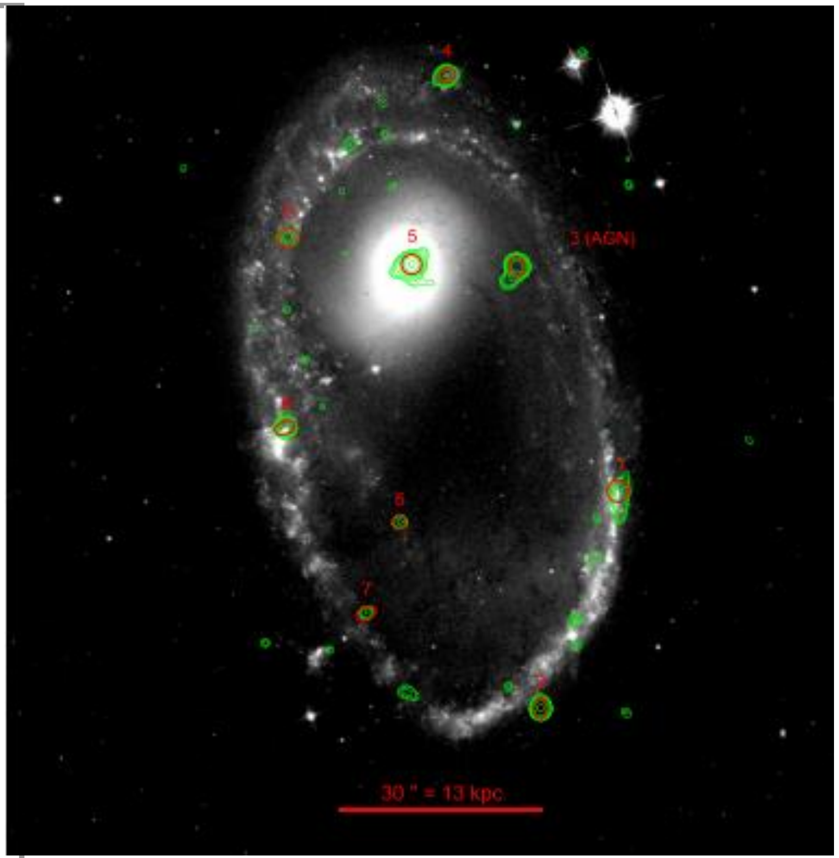

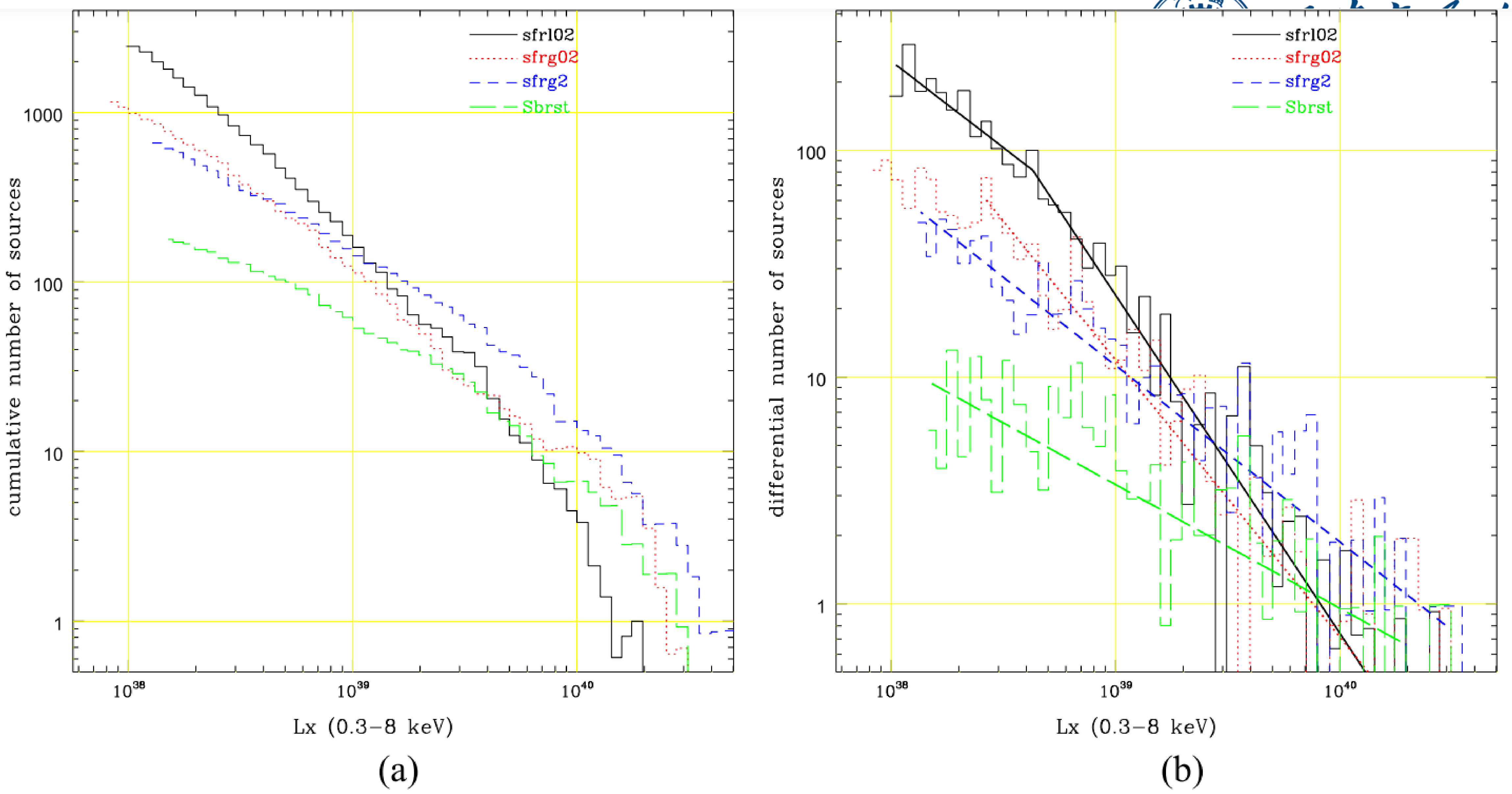

Figure 14. (a) The cumulative curves for the $\mathcal{L}_B$-corrected net nonnuclear sources for galaxies with different SFRs. (b) The differential curves for the $\mathcal{L}_B$-corrected net nonnuclear sources.

附录

星族合成的必要性

The difference between star-burst galaxies and nearby galaxies is obvious in XLF, where the XLF in nearby galaxies show steeper decrease.

Besides, XLF in HMXBs Grimm et al. (2003) was also impossible to fit this in star-burst galaxies. Because the census of these galaxies is not suitable for our simulation for starburst galaxies due to their unique evolution stage and environment.

However, these are requisite for BPS research

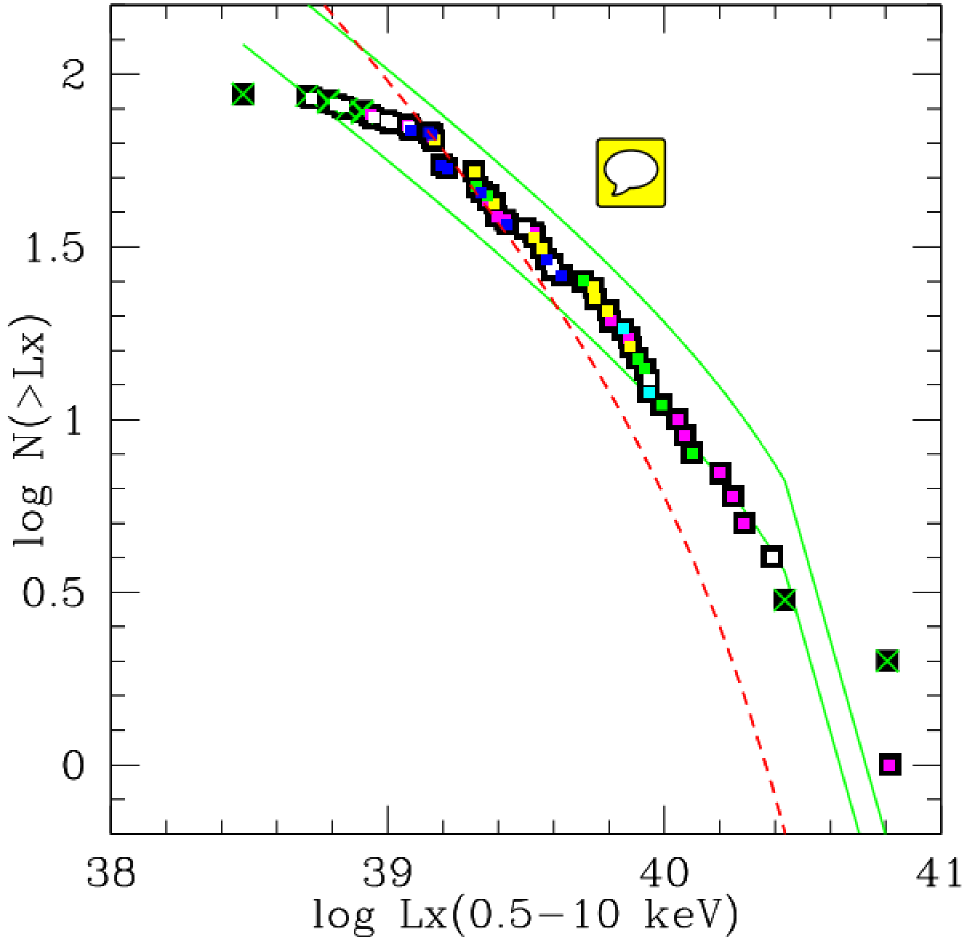

Figure 5. Total X-ray luminosity function (XLF) derived from the seven observed ring galaxies (see the text for details). The green line is the model of Grimm et al. (2003), normalized to SFR = 35 $M_\odot$ yr^{-1} (lower curve), and to 50 $M_\odot$ yr^{-1} (upper curve). The sum of the SFR for the 7 galaxies from Table 2 is 43.5 $M_\odot$ yr^{-1}. Sources with the same color are from the same galaxy. The dashed red line is the model from Swartz et al. (2011) that corresponds to an effective SFR = 50 $M_\odot$ yr^{-1} .

附录

WROF (Abate)

Recently, wind-powered simulation by Baker et al. (2013) demonstrates that the majority of specific ULXs red supergiant companion) transfer mass via wind-fed mode.

the formalism of WRL developed by Abate et al. (2013) was just adoptable for narrow region of parameters, whereas donors stars need to be carbon-enhanced metal-poor stars.

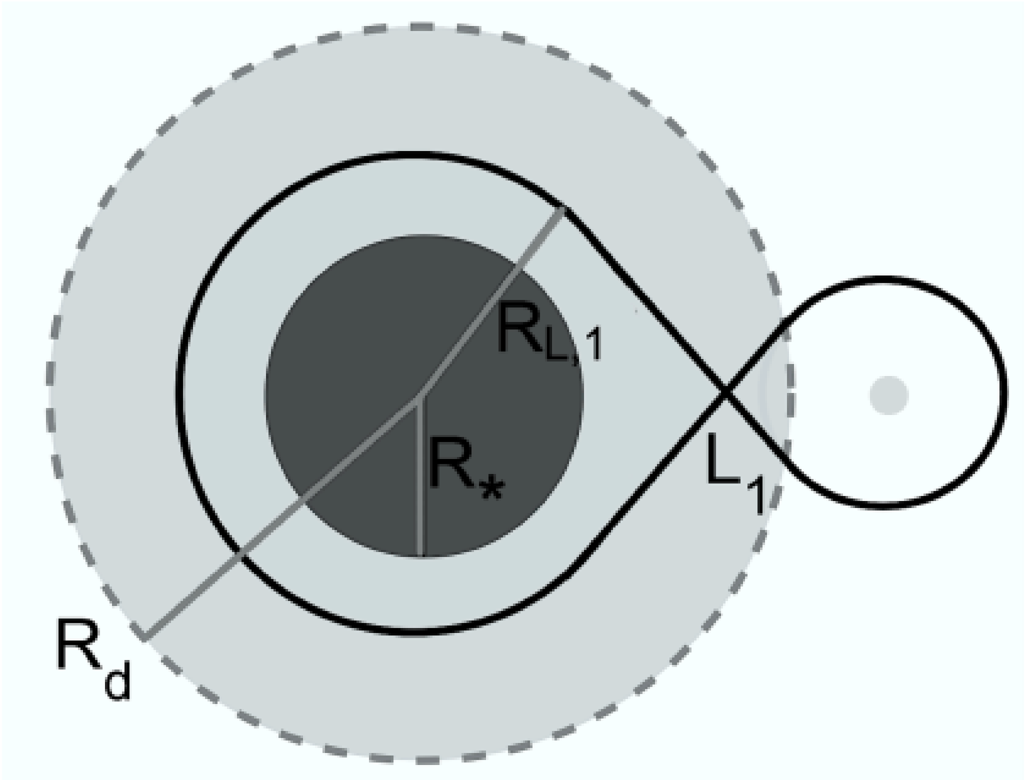

Fig. 1. Schematic picture of the WRLOF mechanism: R_d, the wind acceleration radius, lies close to $R_{L,1}$, the Roche-lobe radius. Inside the wind acceleration zone (shaded area) the wind is slow and can be efficiently accreted to the secondary through the first Lagrangian point L_1 (sizes are not in scale).

附录

WROF (Abate)

1.2−1.8 compared to earlier results that consider the BHL prescription

we allow for the WRLOF MT mode only from donors less massive than 8 M, which is just the maximal mass to which simulations were performed in Mohamed (2010).

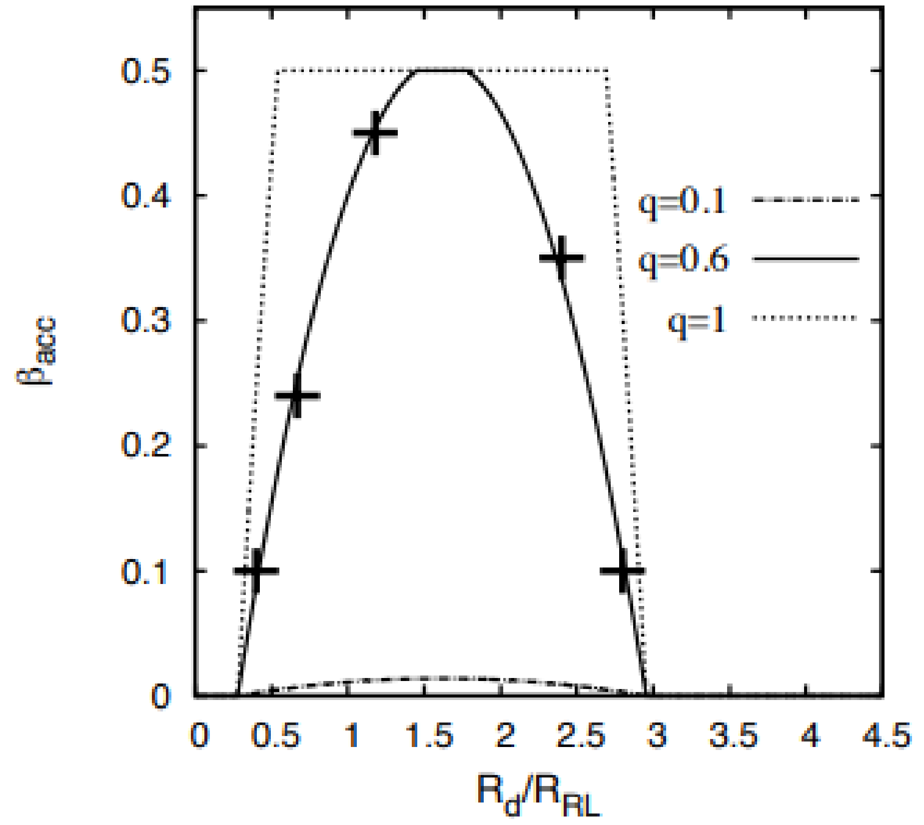

Fig. 2. Models of the wind accretion efficiency β_{acc} for different values of q calculated with Eq. (9). The solid line is for $q = 0.6$, the mass ratio used by Mohamed (2010). The dot-dashed and dotted lines show the resulting efficiency for $q = 0.1$ and $q = 1$, respectively. Plus signs are the results of hydrodynamical simulations by Mohamed (2010) listed in Table 1.

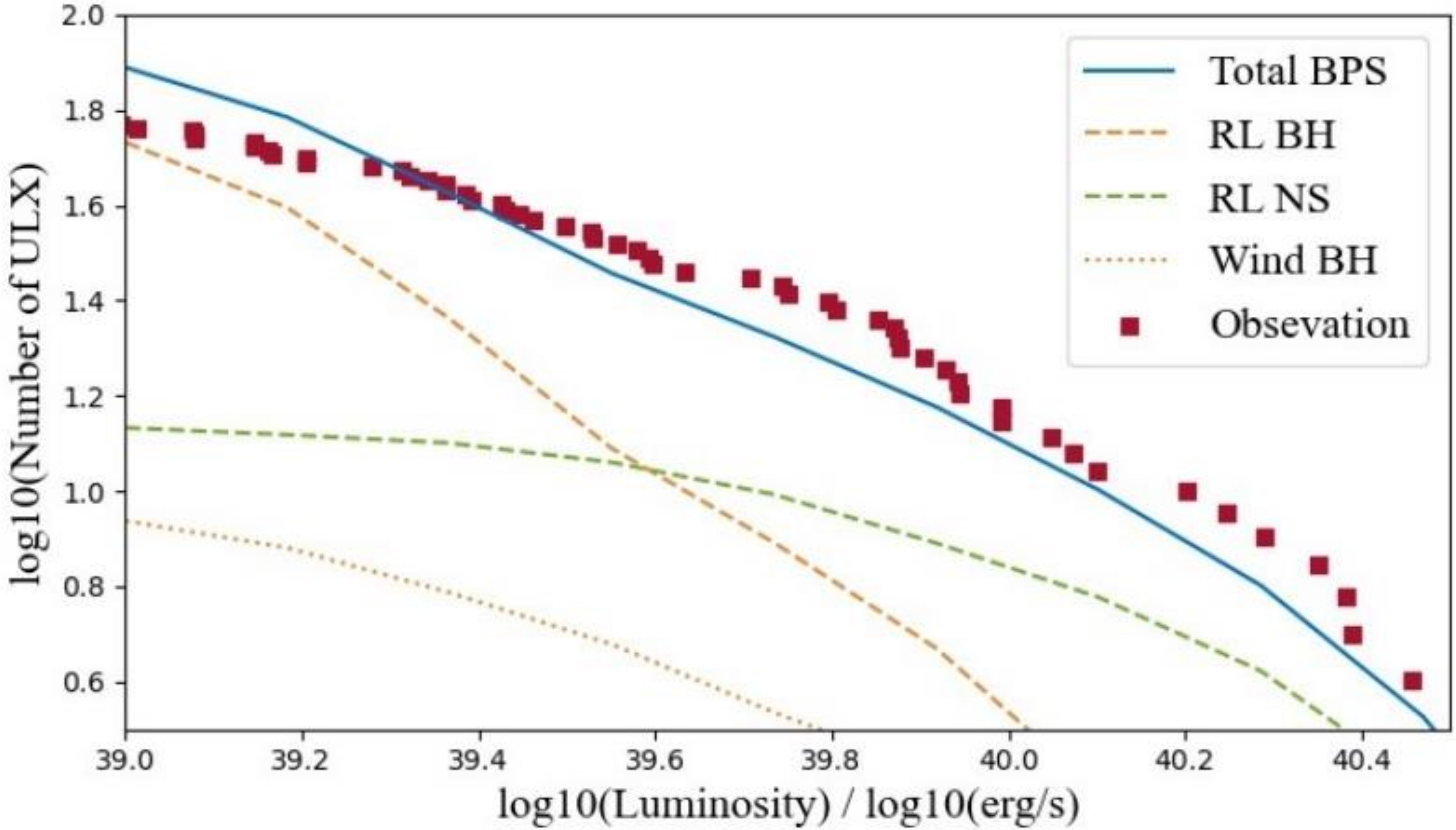

Total BPS
RL BH
RL NS
Wind BH
Obsevation
log10(Number of ULX)
log10(Luminosity) / log10(erg/s)
2.0
1.8
1.6
1.4
1.2
1.0
0.8
0.6
39.0
39.2
39.4
39.6
39.8
40.0
40.2
40.4

附录

XI'AN JIAOTONG UNIVERSITY

Analysis

1, there is a break at approximately 3×10^{40} erg/s which accords with the observation of other galaxies Mineo et al. (2012)

2, Although extreme objects reaching a peak luminosity of 10^{41}erg/s exist (e.g., M82) Gao et al. (2003), they are candidates for Intermediate Mass Black Holes (IMBHs) with masses in between ($10^2 - 10^5$ M) Kuranov et al. (2007); Greene et al. (2020). With completely disparate formation scenarios, IMBHs exclude from consideration in this work.

3, Small probability of forming extremely luminous in our simulation, they demand high beaming factor and correspondingly are impossible to be detected. Additionally, the observation in this region is also limited, so we focus on middle part of XLF

Analysis

ULXs via WRL exist and can reach luminosity at 5×10^{40} erg/s.

吸积效率最大为50%，在我们的模拟中，不超过20%。

In our simulation, high donor star mass and considerable mass transfer rate provide enough fuel for X-ray radiation. For WRL, Roche Lobe is brimming with donor star where situation is unstable in RL overflow. Consequently, mass ratio limit for donor star is more strict in RL overflow than WRL. Baker et al. (2013)

Analysis

For less luminous sources, the compact stars of ULXs tend to be BH instead of NS.

We note that duration of BH RLOF in high luminosity is significantly longer than NS, and, consequently, more likely to be observed.

The mass and radius of NS is lower than BH, and duration of constant mass transfer is harder to maintain before next evolution stage.

The typical orbit period for BH via RLOF is a few days and donor star mass tends to be less than 2.7 solar mass.

Analysis

Meanwhile, NS dominates in the region with higher luminosity $L_{\{app\}} > 10^{40}\mathrm{erg} * s^{-1}$, which is analogous to the previous work {Shao2015}.

In our simulation, there is a proven positive correlation between beaming factor and luminosity.

X-ray radiation in BH ULXs is commonly isotropical or mildly-beamed. However, beaming effects is obvious in NS ULXs, and saturated beaming ($b_{\{\min\}} = 3.2 * 10^{-3}$see \cite{lasota2016slimming}) can be reached in some cases, which is an immediate cause of high luminosity of NS ULXs.